Nonlinear Dynamics of Yaw Motion of Surface Vehicles

Prashant Kambali (prashant.kambali@villanova.edu)
Villanova University College of Engineering https://orcid.org/0000-0003-3826-1233
C. Nataraj
Villanova University College of Engineering

Research Article

Keywords: Surface vehicles, Nonlinear modeling, Bifurcations, Nonlinear dynamics

Posted Date: April 27th, 2022

DOI: https://doi.org/10.21203/rs.3.rs-1515787/v1

Noname manuscript No.
(will be inserted by the editor)

Nonlinear Dynamics of Yaw Motion of Surface Vehicles

Prashant N. Kambali · C. Nataraj

Received: date / Accepted: date

ABSTRACT

The dynamics of surface vehicles such as boats and ships, when modeled as a rigid body, is complex as it is strongly nonlinear and involves six degrees of freedom. We are particularly interested in the steering dynamics decoupled from pitching and rolling as the basis of our research on unmanned boats and autonomy. Steering dynamics has been traditionally modeled using a linear Nomoto model, which however does a poor job of capturing real nonlinear phenomena. On the other hand, there exists a somewhat simplified three degree of freedom nonlinear model derived by Abkowitz, which, although better than the Nomoto model, is still too intractable for analytical methods. In this paper, we derive a nonlinear single degree of freedom model with a cubic nonlinearity that is conditionally equivalent to the Abkowitz model. Using this model we analyze the yaw motion of an autopilot ship with a PD controller under the influence of an external wave force.

Analytical and numerical investigations of the nonlinear dynamics are performed using parameters of an example container ship for various sea states. We employ the harmonic balance method to investigate the nonlinear frequency response of the ship under the influence of different parameters and demonstrate that the external wave force is balanced by stiffer ships. We also numerically investigate the nonlinear dynamic behavior to understand the different mechanisms involved in transitions from periodic to chaotic behavior under the influence of various parameters and different sea state conditions. The analysis reveals periodic response of the ship for a calm sea state. It is noteworthy that for lower values of linear stiffness, higher values of nonlinear stiffness, and higher values of external wave force corresponding to higher sea states, the bifurcation structure reveals mixed dynamic response in which periodic solutions evolve into period doubled, period tripled, and chaotic like solutions even with high levels of damping. This work aims to demonstrate the utility of a simple nonlinear model and nonlinear behavior of

Prashant N. Kambali · C. Nataraj
Villanova Center for Analytics of Dynamic Systems (VCADS)
Villanova University
E-mail: {prashant.kambali, nataraj}@villanova.edu

steering motion of the ships to gain better insight into the nonlinear dynamics of autonomous surface vehicles. Further, the model stands out as an accessible nonlinear model for steering motion of the ship adequately representing the dynamics of real ships. It hence provides a basis for much improved controller design to implement smarter autopilots on manned ships but also aids in the development of robust autonomy in surface vehicles.

Keywords Surface vehicles · Nonlinear modeling · Bifurcations · Nonlinear dynamics

1 INTRODUCTION

The dynamics of a surface vehicle - such as a boat or ship - is generally governed by six degrees of freedom, i.e., three translation motions (surge, sway and yaw) and three rotational motions (roll, pitch and heave). General nonlinear dynamic analysis of ship motions is highly complex and has been investigated by many researchers, especially in pitch and roll, but the reported research is rather sparse in yaw. This paper focuses on the steering motion (and, hence, surge, sway, and yaw) and hence we limit the literature review to only the relevant analyses.

Early studies on the steering dynamics of ships may be traced back to Davidson [1], Nomoto [2], and Abkowitz [3]. The stability of ship autopilots in yaw is discussed by Fossen and Lauvdal [4]. They analyzed the so-called Nomoto model, a simplified linear second order model, and discovered that the ship must move at a minimum speed to remain stable. Fossen and his colleagues at the Norwegian Institute of Technology have conducted more research in this area [5–15].

Hicks et. al. [16] derived realistic hydrodynamic coefficients to analyze the nonlinear dynamics of planning hulls, and they discovered instabilities and bifurcations. Chen, et al. [17] developed a systematic technique for modeling nonlinear ship dynamics in a very comprehensive and outstanding study. However, their focus is on roll, sway, and heave, which is of limited relevance for our current problem. Lefeber and colleagues [18] employed a nonlinear model to achieve tracking control and reported some fascinating findings. However, it is unclear if a simpler model would suffice, or whether a more complicated model is required to achieve their results.

Currently, the above ideas have not been fully demonstrated in naval studies, a field that is primarily dominated by linear concepts. As we know, an understanding of the nonlinear dynamics of surface vehicles enables the identification of the onset, evolution, and often unsafe responses beyond the linear regime that cannot be captured by conventional seakeeping techniques. When the relationship between stimulus and response in a dynamical system is nonlinear, multiple solutions can exist for certain values of the parameters. There are many well-known manifestations of nonlinear behavior, such as unexpected, violent motion that leads to vehicle escape, irregular behavior under regular excitation, subtle boundaries between domains of co-existing responses, and strong sensitivity to initial conditions. As a result, understanding the principles driving nonlinear behavior is imperative for assessing critical behavior.

In numerous cases, nonlinear phenomena have been discovered to underlie ship dynamics, much as they do for the dynamics of other engineering systems [19, 20].

It is shown in [21] that a ship maneuvering problem can be modeled as a motion with three degrees of freedom. However, the roll induced by turning motion is not negligible for high-speed vessels. As a result, a four degree of freedom description is required [22–25], which incorporates surge, sway, and roll modes.

Norrbin [26] proposed a nonlinear model to examine the surge, sway, and yaw motions for ship maneuvering in deep and confined waters, based on both experimental and analytical methods. Fang and Liao [27] demonstrated that nonlinear theory and time domain simulation can be utilized to investigate big ship motions induced by large waves. Spyrou [28] investigated the yaw motion of numerous ships in the presence of a steady wind. He discovered that heading winds can cause Hopf bifurcation, and concluded that most ships are dynamically unstable, requiring active steering to stay on course. Yasukawa et al. [29] concluded that steering control is necessary to reduce the instability of yaw motion of a ship in a steady wind. More recently, Nataraj et.al. [30] proposed a tracking control algorithm for a three degree of freedom steering model by deriving time varying coefficients for the linear error equations. As evidenced by some of the above papers, today's increased computer power does allow us to conduct research based on mathematical models with a high level of detail that can be interesting, but unfortunately these elaborate models offer limited understanding and insight.

The impetus for this study originates from the necessity to build robust and predictable automatic control of surface ships in order to implement autonomous behavior. As a result, a key question to consider at this point is whether the model we chose is acceptable for accurately representing the dynamics of real ships. Until now, the models employed in the literature to assess the yaw motion of autopilot ships have been either very sophisticated or very simple linear models. Complex models are more realistic in their predictions of real ship behavior, but they can be difficult to analyze and regulate. Linear models, on the other hand, such as the Nomoto model, are insufficiently sophisticated to anticipate key occurrences, particularly nonlinear behavior. Therefore, there is a need for a simple model adequately representing the dynamics of real ships, which is the primary goal of this paper. Additionally, such a nonlinear model that is relatively easy to implement and design controllers for would go a long way towards accurate controller design for both manned and unmanned surface vehicles.

Note that what we really want is a model sophisticated enough to include all the critical phenomena, but nothing more complicated than that. That is, we would like to use the simplest model possible that still adequately captures the dynamics. It is hence the intention of this research (i) to derive a simple and yet nonlinear governing equation of yaw motion for an autopilot ship and (ii) to investigate its nonlinear behavior.

The manuscript is organized as follows: In Section 2, we derive a governing equation for the nonlinear yaw motion of a autopilot ship. In Section 3, we seek a solution using the harmonic balance method (HBM). Subsequently, we use the data available in literature and investigate the nonlinear behavior of the ship analytically and numerically in Section 4. Finally, in Section 5, we summarize our findings.

2 MATHEMATICAL MODEL

Fig. 1 depicts a marine vehicle and typical coordinate reference frames. The coordinate system (X_g, Y_g, Z_g) is anchored to the ground with the Z_g axis vertically pointing down. The body-fixed axes (X, Y, Z) are fixed at the vehicle's center of mass, O. The x axis is always parallel to the vehicle's longitudinal symmetry axis (from aft to fore); the y axis is perpendicular to the vehicle (directed to starboard); and the z axis is defined by the cross product. The z axis would be vertically down if the vehicle were horizontal [18].

Surge (u) along the x-axis, sway (v) along the y-axis, heave (w) along the z-axis, and roll (p), pitch (q), and yaw (r) are the six rigid body degrees of freedom of the vehicle. Using angular orientation defined by a sequence of Euler angles (ψ, θ, ϕ), the motion of the vehicle can be specified in body-fixed coordinates or earth-fixed coordinates. The resultant equations are highly complex and have been published in a number of sources, including [30–32].

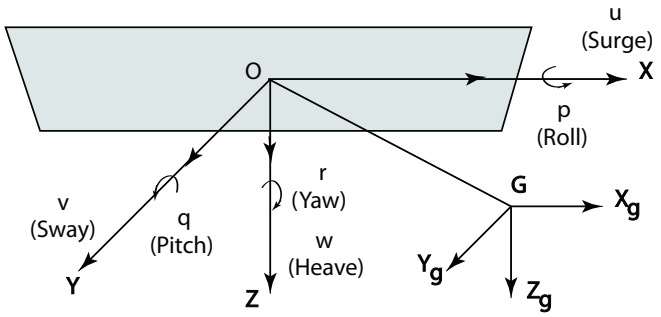

Fig. 1: Boat Model.

The following assumptions are made to decouple the steering dynamics from the surge mode in order to address a restricted problem:

$$p = q = 0, \quad w = 0, \quad \theta = \phi = 0. \tag{1}$$

These assumptions are reasonable when one wants to consider only the yawing motion. Then, the kinematic equations simplify to the following

$$\begin{aligned} \dot{x} &= u\cos\psi - v\sin\psi, \\ \dot{y} &= u\sin\psi + v\cos\psi, \\ \dot{\psi} &= r. \end{aligned} \tag{2}$$

It is to be noted that these equations are nonlinear, despite being simpler than the three-dimensional case. The dynamic equations become

$$\begin{aligned} m\left(\dot{u} - rv\right) &= X, \\ m\left(\dot{v} + ru + x_G\dot{r}\right) &= Y, \\ I_z\dot{r} + mx_G\left(\dot{v} + u_0 r\right) &= N, \end{aligned} \tag{3}$$

where the forces on the RHS arise due to propulsion, actuation, disturbances and hydrodynamics.

In a series of pioneering papers and reports, Abkowitz [33] proposed a third order Taylor series expansion of the forces about a steady operating condition of constant forward speed

$$\begin{aligned} u = u_0 + \bar{p}, \quad v = \bar{v}, \quad w = \bar{w}, \\ p = \bar{p}, \quad q = \bar{q}, \quad r = \bar{r}. \end{aligned} \tag{4}$$

Although this model is not linearized, it is required that perturbations be small; however, note that the steady forward speed, u_0 can be – and is often – a large quantity.

With certain restricted assumptions, the force equations can be described as depicted in Eq. (5). The Taylor series expansion of RHS in Eq. (3) consists of up to third order derivatives. It includes some non-negligible terms such as coupling between the velocity and acceleration, but some other terms are not included because their effect is insignificant in practice. As a matter of notation, note that the terms in the equation include the numerical factor of $1/n!$, for example, $X_{uu} = \frac{1}{2!}\frac{\partial^2 X}{\partial u^2}$.

$$\begin{aligned} X &= X_0 + X_{\dot{u}}\dot{u} + X_u\bar{u} + X_{uu}\bar{u}^2 + X_{vv}\bar{v}^2 + X_{rr}\bar{r}^2 + X_{\delta\delta}\delta^2 \\ &\quad + X_{rv}\bar{r}\bar{v} + X_{r\delta}r\delta + X_{v\delta}\bar{v}\delta + X_{uuu}\bar{u}^3 + X_{vvu}\bar{v}^2\bar{u} + X_{rru}\bar{r}^2\bar{u} \\ &\quad + X_{\delta\delta u}\delta^2\bar{u} + X_{rvu}\bar{r}\bar{v}\bar{u} + X_{r\delta u}\bar{r}\delta\bar{u} + X_{v\delta u}\bar{v}\delta\bar{u}, \\ Y &= Y_0 + Y_u\bar{u} + Y_v\bar{v} + Y_r\bar{r} + Y_\delta\delta + Y_{\dot{v}}\dot{\bar{v}} + Y_{\dot{r}}\dot{\bar{r}} + Y_{uu}\bar{u}^2 + Y_{vu}\bar{v}\bar{u} + Y_{ru}\bar{r}\bar{u} + Y_{\delta u}\delta\bar{u} \\ &\quad + Y_{vvv}\bar{v}^3 + Y_{rrr}\bar{r}^3 + Y_{\delta\delta\delta}\delta^3 + Y_{rr\delta}\bar{r}^2\delta + Y_{\delta\delta r}\delta^2\bar{r} + Y_{rrv}\bar{r}^2\bar{v} \\ &\quad + Y_{vvr}\bar{v}^2\bar{r} + Y_{\delta\delta v}\delta^2 v + Y_{vv\delta}\bar{v}^2\delta + Y_{\delta vr}\delta\bar{v}\bar{r} + Y_{vuu}\bar{v}\bar{u}^2 + Y_{ruu}r\bar{u}^2 \\ &\quad + Y_{\delta uu}\delta\bar{u}^2, \\ N &= N_0 + N_u\bar{u} + N_v\bar{v} + N_r\bar{r} + N_\delta\delta + N_{\dot{v}}\dot{\bar{v}} + N_{\dot{r}}\dot{\bar{r}} + N_{uu}\bar{u}^2 + N_{vu}\bar{v}\bar{u} + N_{ru}\bar{r}\bar{u} + N_{\delta u}\delta\bar{u} \\ &\quad + N_{vvv}\bar{v}^3 + N_{rrr}\bar{r}^3 + N_{\delta\delta\delta}\delta^3 + N_{rr\delta}\bar{r}^2\delta + N_{\delta\delta r}\delta^2\bar{r} + N_{rrv}\bar{r}^2\bar{v} \\ &\quad + N_{vvr}\bar{v}^2\bar{r} + N_{\delta\delta v}\delta^2\bar{v} + N_{vv\delta}\bar{v}^2\delta + N_{\delta vr}\delta\bar{v}\bar{r} + N_{vuu}\bar{v}\bar{u}^2 + N_{ruu}r\bar{u}^2 \\ &\quad + N_{\delta uu}\delta\bar{u}^2. \end{aligned} \tag{5}$$

Eq. (3) represents a three-DOF nonlinear model that is practically applicable to most surface vehicles when these forces are incorporated. The definition of various notations in Eq. (5) are given in Appendix.

2.1 Linearized Model

In this subsection, for comparison, we linearize the forces in Eq. (5) for the special case of constant speed forward motion assuming small perturbations. And the hydrodynamic forces then take the following form

$$\begin{aligned} X &= X_0 + X_{\dot{u}}\dot{\bar{u}} + X_u\bar{u}, \\ Y &= Y_0 + Y_u\bar{u} + Y_v\bar{v} + Y_r\bar{r} + Y_\delta\delta + Y_{\dot{v}}\dot{\bar{v}} + Y_{\dot{r}}\dot{\bar{r}}, \\ N &= N_0 + N_u\bar{u} + N_v\bar{v} + N_r\bar{r} + N_\delta\delta + N_{\dot{v}}\dot{\bar{v}} + N_{\dot{r}}\dot{\bar{r}}. \end{aligned} \tag{6}$$

The LHS in Eq. (3) also simplifies as follows

$$\begin{aligned} m\dot{\bar{u}} &= X + X_T, \\ m\left(\dot{\bar{v}} + u_0\bar{r} + x_G\dot{\bar{r}}\right) &= Y, \\ I_Z\dot{\bar{r}} + mx_G\left(\dot{\bar{v}} + u_0 r\right) &= Z. \end{aligned} \tag{7}$$

Applying steady-state conditions and reasonably assuming that the thrust of the propeller balances out the losses and hydrodynamic forces under constant speed condition, we can drop the constant terms in the RHS, as well as u terms to get

$$\begin{aligned} &(m - Y_{\dot{v}})\,\dot{\bar{v}} + (mx_g - Y_{\dot{r}})\,\dot{\bar{r}} - Y_v\bar{v} + (mu_0 - Y_r)\,\bar{r} = Y_\delta\delta, \\ &(I_Z - N_{\dot{r}})\,\dot{\bar{r}} + (mx_G - N_{\dot{v}})\,\dot{\bar{v}} - N_v\bar{v} + (mx_G u_0 - N_r)\,\bar{r} = N_\delta\delta. \end{aligned} \tag{8}$$

Next, eliminating v from the above equations leads to the following equation often called Nomoto's 2$^{\text{nd}}$ order model [2]

$$T_1T_2\dddot{\psi} + (T_1 + T_2)\ddot{\psi} + \dot{\psi} = K\left(\delta + T_3\dot{\delta}\right), \tag{9}$$

where T_1, T_2, T_3, and K are constants given by Eqs. (27)-(33) in Appendix which depend on parameters due to propulsion, actuation, disturbances, hydrodynamics, surge velocity, and dimensions of the ship. This is the simplest steering model one could employ [2] and is used for most autopilot analysis and design.

Next, we design an autopilot with a proportional plus derivative (PD) controller for above model where the rudder angle, the control input, is given by $\delta = k_p\dot{\psi} + k_d\ddot{\psi}$ [32]. Substituting in Eq. (9) yields the following equation

$$\left(1 - \frac{K}{T_1T_2}k_dT_3\right)\dddot{\psi} + \left[\left(\frac{1}{T_1} + \frac{1}{T_2}\right) + \frac{K}{T_1T_2}\left(k_pT_3 - k_d\right)\right]\ddot{\psi} + \frac{1}{T_1T_2}\left(1 + k_pK\right)\dot{\psi} = 0. \tag{10}$$

Eq. (10) represents a generalized linearized steering model with PD controller which is applicable for ships and boats. In order to continue the numerical analysis, we consider the experimentally validated parameters of a container ship from the literature [22, 34] and are given in Table 1 in the Appendix. Subsequently, we evaluate T_1, T_2, T_3, and K using Eqs. (27)-(33) and parameters in Table 1 and are tabulated in Tab. 2 in the Appendix. For the above equation, we determine the controller gains using MATLAB$^{\text{TM}}$ Control System toolbox [35]. We designed the linearized system to achieve a settling time of 90 seconds and an overshoot of 15%. This results in the following values for the controller gains: $k_p = 1.9$ and $k_d = 0.1986$.

Note that Eq. (9) is obtained by linearizing the equations of motion around the zero rudder angle. As a result, the rudder angle should not exceed approximately 5 degrees, otherwise, the model would be inaccurate. So, we need a model that is suitable for rudder angles that are larger than 5 degrees and can also describe the ship's behavior for a wide range of manoeuvres. For this purpose, the coefficients T_1, T_2, T_3, and K are made functions of the instantaneous values of $\dot{\psi}$ and δ. As a result, we substitute $\frac{1}{K}\dot{\psi} = H(\dot{\psi})$ in Eq. (9) yielding

$$\dddot{\psi} + \left(\frac{1}{T_1} + \frac{1}{T_2}\right)\ddot{\psi} + \frac{K}{T_1T_2}H(\dot{\psi}) = \frac{K}{T_1T_2}[T_3\dot{\delta} + \delta], \tag{11}$$

where $H(\dot{\psi})$ is a nonlinear function of $\dot{\psi}$ describing the maneuvering characteristic [36], which also ensures correct steady turn solutions. $H(\dot{\psi})$ can be found from the relationship between δ and $\dot{\psi}$ in steady state such that $\dddot{\psi} = \ddot{\psi} = \dot{\delta} = 0$. The expression for $H(\dot{\psi})$ is obtained by fitting the $\dot{\psi} - \delta$ curve in Fig. 2 obtained by numerically solving the Abkowitz model [33] (Eqs. (2), (3), (5)) using parameters given in Tab. 1 in the Appendix. The expression for $H(\dot{\psi})$ is as follows.

$$H(\dot{\psi}) = a\dot{\psi} + b\dot{\psi}^2 + c\dot{\psi}^3 + d. \tag{12}$$

where, $a = 1.6$, $b = -0.052$, $c = 2.7$ and $d = -0.00057$.

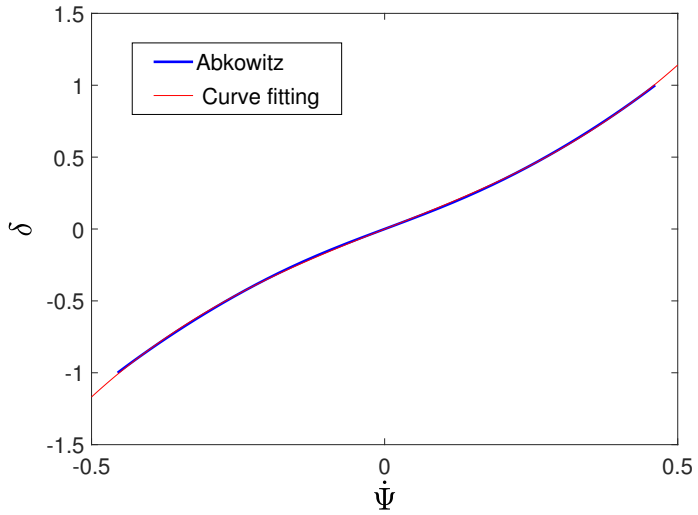

Fig. 2: Curve fit for $H(\dot{\psi})$ for the ship. In this case results represented by blue color indicates numerical solutions obtained by Abkowitz model [33].

Ship response to waves is generally of great importance in evaluating the sea keeping performance of the ship. The forces and moments exerted by the sea waves also greatly influence the steering dynamics. To account for the influence of the waves, in the simplest case, it may be assumed that the waves incident upon the body are plane progressive waves of small amplitude with sinusoidal time dependence. Hence we can represent the wave force N_w as

$$N_w(t) = f\cos(\bar{\Omega}\bar{t}). \tag{13}$$

Note that the wave amplitude in Eq. (13) is proportional to the sea states. Sea state is the state of oscillation of the sea surface (waves) generated by wind energy and is defined as the mean wave height. The various sea states and the corresponding range of wave heights is documented in [37].

Combining Eqs. (10),(11),(12),(13) the nonlinear steering model of USVs in the yaw direction under external wave force is given by

$$\Big(1-\frac{K}{T_1T_2}k_dT_3\Big)\dddot{\psi}+\left[\Big(\frac{1}{T_1}+\frac{1}{T_2}\Big)+\frac{K}{T_1T_2}\left(k_pT_3-k_d\right)\right]\ddot{\psi}+\frac{K}{T_1T_2}\left(a+k_p\right)\dot{\psi}$$
$$+b\frac{K}{T_1T_2}\dot{\psi}^2+c\frac{K}{T_1T_2}\dot{\psi}^3+d\frac{K}{T_1T_2}=f\cos(\bar{\Omega}\bar{t}), \qquad (14)$$

Substituting yaw rate, r for $\dot{\psi}$ and rewriting Eq. (14),

$$a_{11}\ddot{r}+a_{12}\dot{r}+a_{13}r+a_{14}r^2+a_{15}r^3+a_{16}=f\cos(\bar{\Omega}\bar{t}), \qquad (15)$$

where, $a_{1i}\,(i=1...6)$ are given by Eq. (34) in the Appendix. We rescale Eq. (15) by $r=y/a_{15}^{1/3}-a_{14}/3a_{15}$ and after simplification, the resulting equation is

$$a_{11}\ddot{y}+a_{12}\dot{y}+b_{11}y+a_{15}{}^{\frac{1}{3}}y^3+b_{12}=f\cos(\bar{\Omega}\bar{t}), \qquad (16)$$
$$b_{11}=\left(a_{13}-\frac{a_{14}^2}{3a_{15}}\right),\qquad b_{12}=\left(a_{16}-\frac{a_{13}a_{14}}{3a_{15}}+\frac{2a_{14}^3}{27a_{15}^2}\right)a_{15}^{\frac{1}{3}},\qquad b_{13}=fa_{15}^{\frac{1}{3}}.$$

Finally, we nondimensionalize Eq. (16) using $t=\omega\bar{t}$ where $\omega=\sqrt{b_{11}}$ and the resulting equation with nondimensional parameters is as follows:

$$\ddot{y}+\gamma\dot{y}+\alpha_1y+\alpha_2y^3+\Delta=F\cos(\Omega t), \qquad (17)$$
$$\gamma=\frac{a_{12}}{a_{11}\sqrt{b_{11}}},\ \alpha_1=\frac{1}{a_{11}},\ \alpha_2=\frac{a_{15}^{\frac{1}{3}}}{a_{11}b_{11}},\ \Delta=\frac{b_{12}}{a_{11}b_{11}},\ F=\frac{b_{13}}{a_{11}b_{11}}.$$

Finally, Eq. (17) represents a nonlinear steering model in the yaw direction and resembles a Duffing-like oscillator. In the next section, we seek an approximate solution using harmonic balance method (HBM) for above equation that importantly retains strong nonlinearity.

3 Harmonic Balance Method

In this section, we apply the harmonic balance method (HBM) [38] to Eq. (17) to get approximate solutions. We assume a solution with only one harmonic as

$$y(t)=A_c\cos(\Omega t)+A_s\sin(\Omega t). \qquad (18)$$

Substituting Eq. (18) into Eq. (17), using the trigonometric identities for $\cos(\Omega t)^3$, $\sin(\Omega t)^3$, $\cos(\Omega t)^2$ and $\sin(\Omega t)^2$ and collecting the harmonics results in

$$\left[\Big(\alpha_1-\Omega^2\Big)A_c+\gamma\Omega A_s+\frac{3}{4}\alpha_2\Big(A_c^3+A_cA_s^2\Big)-F\right]\cos(\Omega t)+\left[\Big(\alpha_1-\Omega^2\Big)A_s-\gamma\Omega A_c\right.$$
$$\left.+\frac{3}{4}\alpha_2\Big(A_s^3+A_sA_c^2\Big)\right]\sin(\Omega t)+hh(3)=0, \qquad (19)$$

where $hh(3)$ denotes third and higher harmonics. Equating to zero the coefficients of $\cos \Omega t$ and $\sin \Omega t$ in Eq. (19), respectively, yields

$$\Big(\alpha_1 - \Omega^2\Big)A_c + \gamma\Omega A_s + \frac{3}{4}\alpha_2\Big(A_c^3 + A_c A_s^2\Big) - F = 0,$$
$$\Big(\alpha_1 - \Omega^2\Big)A_s - \gamma\Omega A_c + \frac{3}{4}\alpha_2\Big(A_s^3 + A_s A_c^2\Big) = 0. \tag{20}$$

We choose $A_c = a\cos\theta$ and $A_s = a\sin\theta$ such that $A_c^2 + A_s^2 = a^2$ and substitute in Eq. (20) which results in

$$\Big(\alpha_1 - \Omega^2\Big)a\cos\theta + \gamma\Omega a\sin\theta + \frac{3}{4}\alpha_2\Big(a^3\cos\theta^3 + \cos\theta a^2\sin\theta^2\Big) = F, \tag{21}$$
$$\Big(\alpha_1 - \Omega^2\Big)a\sin\theta - \gamma\Omega a\cos\theta + \frac{3}{4}\alpha_2\Big(a^3\sin\theta^3 + a\sin\theta a^2\cos\theta^2\Big) = 0. \tag{22}$$

After algebraic manipulation of Eqs. (21) and (22), we set

$$\Big(\alpha_1 - \Omega^2\Big)a + \frac{3}{4}\alpha_2 a^3 = F\cos\theta, \tag{23}$$
$$\gamma\Omega a = F\sin\theta. \tag{24}$$

Squaring and adding Eqs. (23) and (24) yields amplitude frequency relationship as

$$\left[\Big(\alpha_1 - \Omega^2\Big) + \frac{3}{4}\alpha_2 a^2\right]^2 a^2 + \gamma^2\Omega^2 a^2 = F^2. \tag{25}$$

Solving Eq. (25) for Ω results in the following frequency response equation

$$\Omega_{1,2}^2 = \alpha_1 - \frac{\gamma^2}{2} + \frac{3\alpha_2 a^2}{4} \pm \sqrt{\frac{F^2}{a^2} + \frac{\gamma^2}{4} - \gamma^2 - \frac{3\gamma^2\alpha_2 a^2}{4}}. \tag{26}$$

4 Results and Discussions

In this section, we investigate the nonlinear behavior of the yaw motion of a ship derived above. As explained in the previous section, this paper considers an example of a container ship and the various experimentally determined nondimensional parameters for the container ship as documented in [22, 34] given in Table. 1 in the Appendix. These parameters depend on the propulsion, actuation, disturbances, hydrodynamics, surge velocity and dimensions of the ship. The constants of Nomoto's second-order model for the container ship are calculated using Eqs. (27)-(33) for parameters in Table 1 and are presented in Table 2 in the Appendix. The nondimensional amplitudes F of the sea wave calculated for different sea states are in Table 3.

We evaluate the nondimensional parameters in Eq. (17) $\gamma = 0.0228$, $\alpha_1 = 0.6457$, $\alpha_2 = 0.0717$, $\Delta = 0.01$ and $F = 2.66f$. Note that any changes in α_1, α_2, and Δ result from changes in parameters mentioned above as well as controller gains whereas changes in F account for changes in amplitudes of the external wave force for different sea states.

4.1 Frequency Response using HBM

We solve Eq. (25) (using MATCONT [39]) or Eq. (26) for the frequency response for various parameters. Fig. 3(a) depicts the frequency response for parameters $\gamma = 0.0228$, $\alpha_1 = 0.6457$, $\alpha_2 = 0.0717$ and $F = 0.0143$, 0.0358 (smooth and slight sea states, see Tab. 3 in Appendix). To analyze the stability of the solution, we compute the Jacobian matrix and eigenvalues associated with Eq. (25).

The equilibrium solution Eq. (25) is stable when $Re(\lambda) < 0$; otherwise, the solution becomes unstable. Fig. 3(b) corresponds to eigenvalues versus Ω for parameters $\gamma = 0.0228$, $\alpha_1 = 0.6457$, $\alpha_2 = 0.0717$ and $F = 0.0358$. In both the figures the blue solid lines indicate stable solutions ($Re(\lambda) < 0$ in Fig. 3(b)) and the red dotted lines indicate unstable solutions ($Re(\lambda) > 0$ in Fig. 3(b)). The red circles in Fig. 3(a) are solutions from numerical simulation of Eq. (17) which are in good agreement with the solutions of HBM.

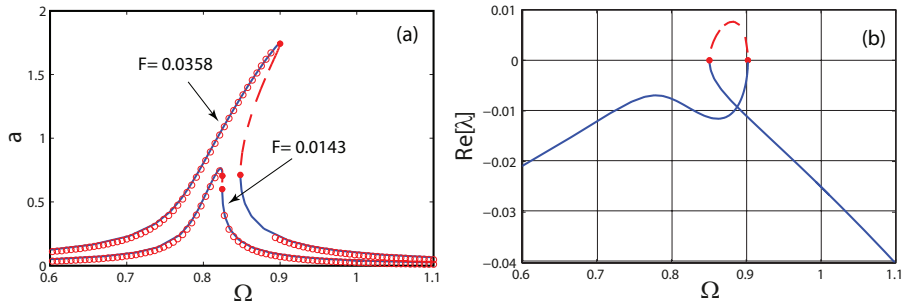

Fig. 3: (a) Frequency response of a container ship for $\gamma = 0.0228$, $\alpha_1 = 0.6457$, $\alpha_2 = 0.071$, $F = 0.0143$ and 0.0358. (b) Stability plot showing eigen values versus Ω for $\gamma = 0.0228$, $\alpha_1 = 0.6457$, $\alpha_2 = 0.071$, $F = 0.0358$. The blue solid lines indicate stable solutions and the red dotted lines indicate unstable solutions from HBM method. The red circles indicates solutions from numerical simulations of Eq. (17).

Frequency response for the same external wave force corresponding to moderate and very rough sea states ($F = 0.08, 0.2$) and damping ($\gamma = 0.05$) and for different values of α_1 and α_2 are shown in Fig. 4(a) (for $\alpha_1 = 0.1$ and $\alpha_2 = 0.5$) and Fig. 4(b) (for $\alpha_1 = 0.5$ and $\alpha_2 = 0.8$). It is observed that for the same external wave force and for the same damping, with an increase in α_1 from 0.1 to 0.5 and α_2 from 0.5 to 0.8, the amplitude of frequency response reduces considerably. This is because with the increase in α_1 and α_2, the ship becomes stiffer and overcomes the external wave force.

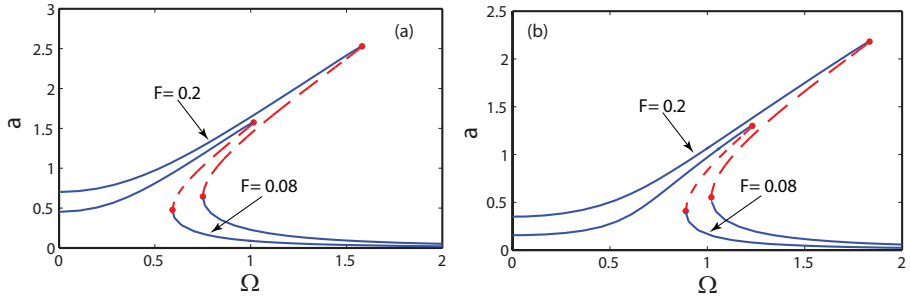

Fig. 4: Frequency response of a container ship for $\gamma = 0.05$ (a) $\alpha_1 = 0.1$, $\alpha_2 = 0.5$ and (b) $\alpha_1 = 0.5$, $\alpha_2 = 0.8$. The blue solid lines indicate stable solutions and the red dotted lines indicate unstable solutions from HBM method.

4.2 Numerical Analysis

Next, we study the nonlinear behavior of the container ship by numerically integrating Eq. (17) and investigate the bifurcation of the system under the effect of various parameters leading to various patterns of behavior including chaos.

Fig. 5(a) depicts the frequency response for the parameters $\gamma = 0.0228$, $\alpha_1 = 0.6457$, $\alpha_2 = 0.071$, $\Delta = 0.0106$, $F = 0.0358$ (slight sea state, see Tab. 3). Figs. 5(b), (c) and (d) shows the time history, phase plane with Poincaré point and power spectra of a periodic motion for $\omega = 0.85$. Under this condition, the system remains periodic throughout the frequency range of $\Omega = 0.5$ to 1.1 as shown by time history, phase plane, and power spectra in Figs. 5(b), (c) and (d). Therefore, under this operating condition and for a slight sea state, we can conclude that the container ship operates safely.

The bifurcation diagram for the parameters $\gamma = 0.05$, $\alpha_1 = 0.1$, $\alpha_2 = 0.5$, $\Delta = 0.01$, and $F = 0.2$ is shown in Fig. 6(a). For this case of a very rough sea state, the bifurcation diagram shows the transition of periodic motions to period doubled and period tripled motions. Time history, phase plane with Poincaré points, and power spectra of period doubling and period tripling motions for $\Omega = 0.86$ and $\Omega = 1.2$ corresponding to Fig. 6(a) are respectively shown in Figs. 7(a)-(f).

The dynamic behavior becomes more complex for a very high sea state for the parameters $\gamma = 0.05$, $\alpha_1 = 0.1$, $\alpha_2 = 0.5$, $\Delta = 0.01$, $F = 0.5$ and the bifurcation diagram is depicted in Fig. 6(b). It is observed from Fig. 6(a) that bifurcation diagram illustrates the transition of chaotic (Ω =0.3255) to period tripling (Ω =0.633), period doubling (Ω =1.1) and periodic solutions (Ω =1.8). Time history, phase plane with Poincaré points and power spectra for chaotic (Ω =0.3255), period tripling (Ω =0.633), period doubling (Ω =1.1) and periodic solutions (Ω =1.8) corresponding to Fig. 6(b) are depicted in Figs. 8(a)-(d), 9(a)-(d), 10(a)-(d), respectively.

Note that, for low linear stiffness, considerably high damping, and high nonlinear stiffness, the steering dynamics of the container ship becomes complex under a very rough sea state condition leading to more complex dynamics for the case of a very high sea state.

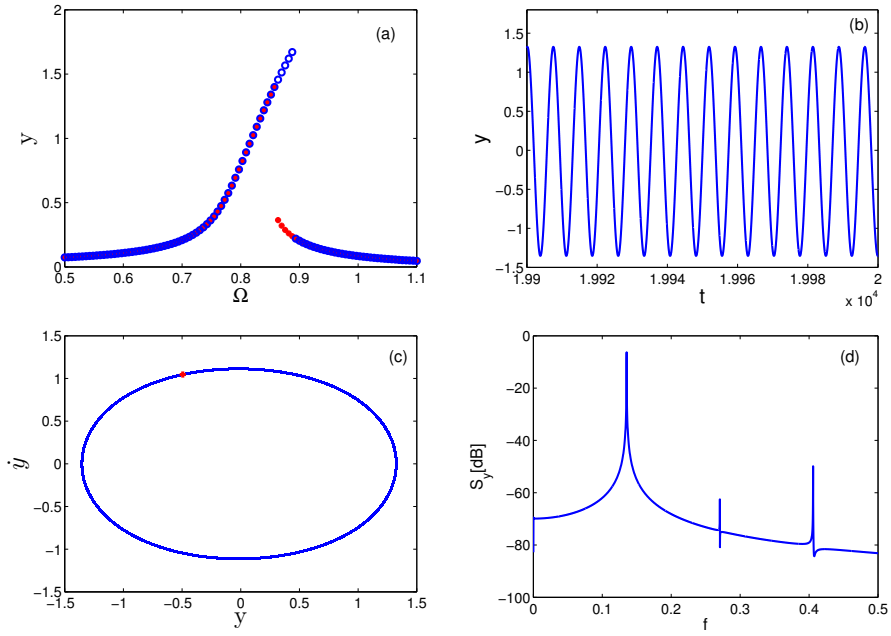

Fig. 5: Numerical simulation of Eq. (17) for a container ship for $\gamma = 0.0228$, $\alpha_1 = 0.6457$, $\alpha_2 = 0.071$, $\Delta = 0.0106$, $F = 0.0358$. (a) Frequency response curve (b) Time history for $\Omega = 0.85$ (c) Phase plane with Poincaré point for $\Omega = 0.85$ and (d) Power spectra for $\Omega = 0.85$. In (a), the blue circles and red asterisk indicates forward and backward numerical solutions.

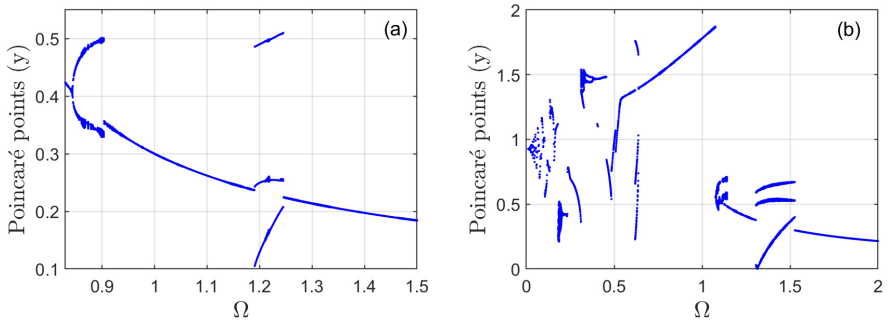

Fig. 6: Bifurcation diagram showing Poincaré points versus Ω for $\gamma = 0.05$, $\alpha_1 = 0.1$, $\alpha_2 = 0.7$, $\Delta = 0.01$, (a) $F = 0.2$ (b) $F = 0.5$.

Fig. 11 shows the bifurcation diagram of the container ship for (a) $\gamma = 0.03$, $\alpha_1 = 0.05$, $\alpha_2 = 0.7$, $\Delta = 0.01$, $F = 0.3$, (b) $\gamma = 0.05$, $\alpha_1 = 0.05$, $\alpha_2 = 0.7$, $\Delta = 0.01$, $F = 0.6$. It is observed from Fig. 11(a) that the steering dynamics of the container ship is very complex with lower values of damping, and linear stiffness and with slightly higher value of nonlinear stiffness for the case of a high sea state

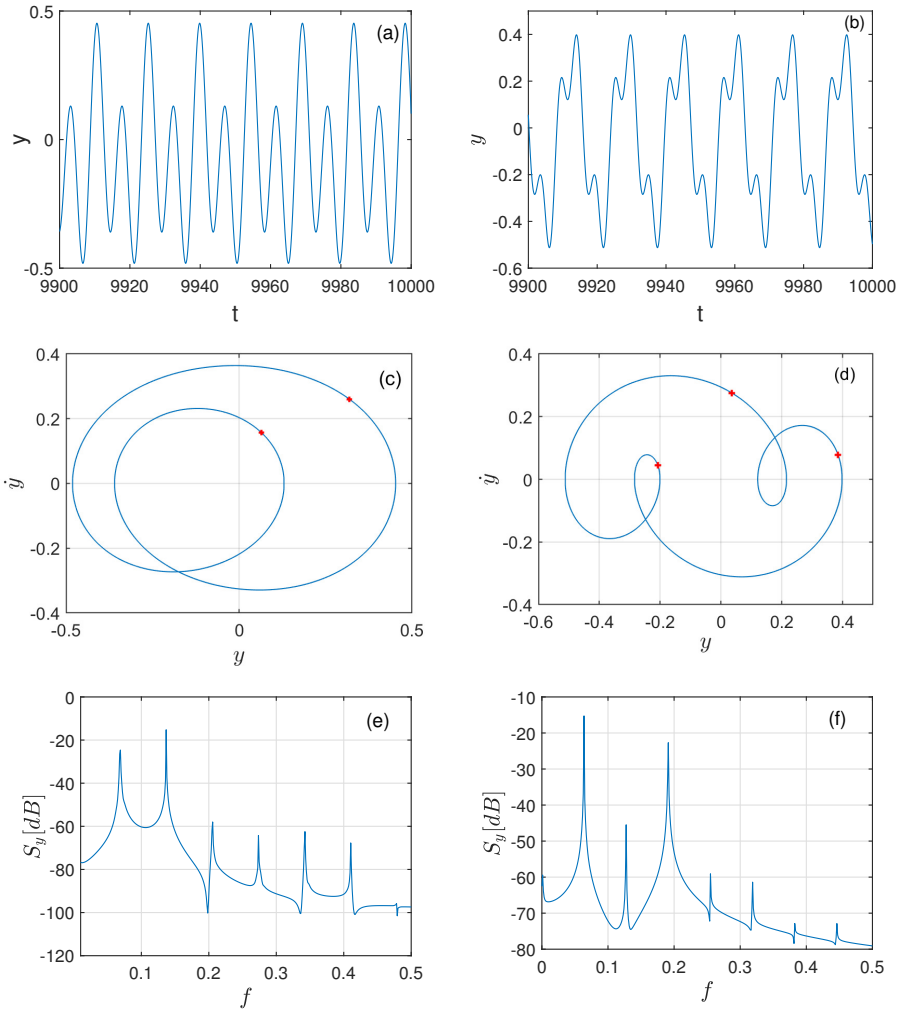

Fig. 7: Time history (a) $\Omega = 0.86$ (b) $\Omega = 1.2$, Phase plane with Poincaré points (c) $\Omega = 0.86$ (b) $\Omega = 1.2$, Power spectra (e) $\Omega = 0.86$ (f) $\Omega = 1.2$ of a numerical simulation of Eq. (17) for a container ship corresponding to Ω =0.86 and 1.2 in Fig. 6(a). In this case $\gamma = 0.05$, $\alpha_1 = 0.1$, $\alpha_2 = 0.5$, $\Delta = 0.01$, $F = 0.2$.

condition. Under a phenomenal sea state condition the complexity increases even for higher values of damping as shown in Fig. 11(b).

5 Closing remarks

Surface vehicles - such as boats and ships - have been designed and used for a very long time in human history. However, their physics and complexity of behavior is still not quite understood. This is because their dynamics even when modeled as

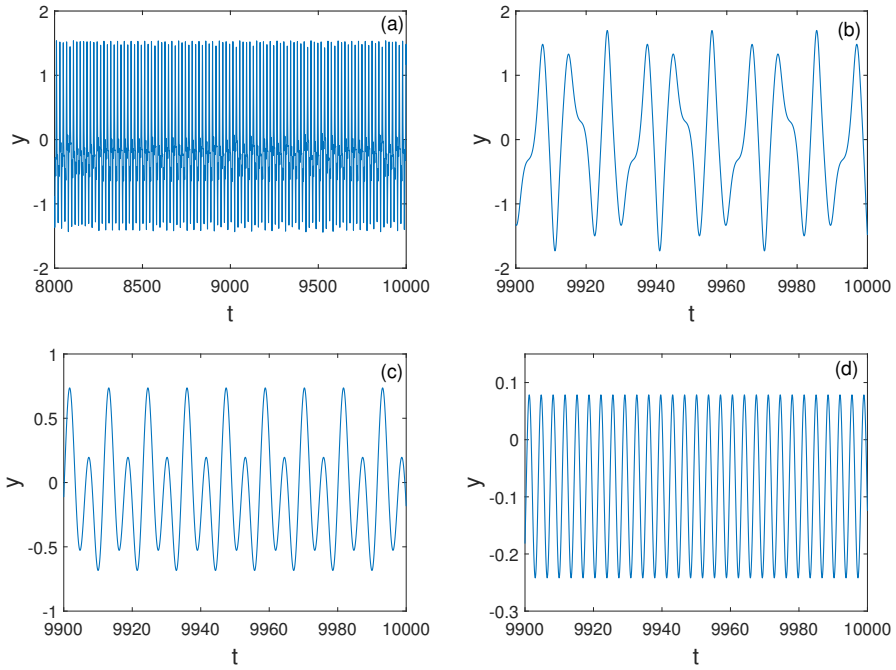

Fig. 8: Time history of a numerical simulation of Eq. (17) for a container ship for $\gamma = 0.05$, $\alpha_1 = 0.1$, $\alpha_2 = 0.5$, $\Delta = 0.01$, $F = 0.5$ corresponding to (a) $\Omega = 0.3255$ (b) $\Omega = 0.633$ (c) $\Omega = 1.1$ (d) $\Omega = 1.8$ in Fig. 6(b).

a rigid body, is strongly nonlinear and would normally include six coupled degrees of freedom. Rolling and pitching motion has received a lot of research attention over the years. While all of the dynamics is interesting and important, we are particularly interested in the steering dynamics when approximately decoupled from pitching and rolling. This is because steering becomes most important for path planning of boats which has been a focus of our research on unmanned boats and autonomy.

Steering dynamics has been traditionally modeled using a linear Nomoto model, which however does a poor job of capturing real nonlinear phenomena. On the other hand, there exists a somewhat simplified three degree of freedom nonlinear model derived by Abkowitz, which, although better than the Nomoto model, is still too intractable for analytical methods. Hence, in our quest for an analytically manageable model we have derived a nonlinear single degree of freedom governing equation with a cubic nonlinearity to represent the yaw motion of an autopilot ship integrated with a PD controller under the influence of an external wave force. The model is conditionally equivalent to the Abkowitz model, a three degree of freedom nonlinear steering model. Our model provides an accessible nonlinear model for steering motion of the ship adequately representing the dynamics of real ships. The nonlinearity in the model is introduced by a nonlinear function of the yaw rate into Nomoto's 2^{nd} order model which is obtained by comparing the Abkowitz model.

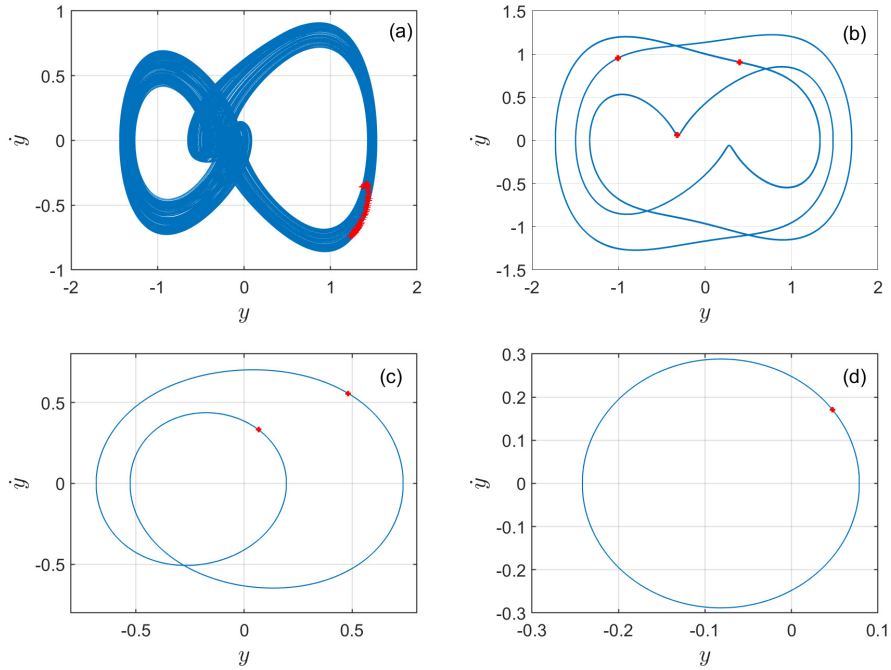

Fig. 9: Phase plane with Poincaré points of a numerical simulation of Eq. (17) for a container ship for $\gamma = 0.05$, $\alpha_1 = 0.1$, $\alpha_2 = 0.5$, $\Delta = 0.01$, $F = 0.5$ corresponding to (a) $\Omega = 0.3255$ (b) $\Omega = 0.633$ (c) $\Omega = 1.1$ (d) $\Omega = 1.8$ in Fig. 6(b).

Using the parameters of an example container ship from the literature [22,34], we investigated the nonlinear dynamics analytically and numerically. We employed the harmonic balance method (HBM) to study the nonlinear frequency response under the influence of external wave force, linear, nonlinear stiffness, and damping. From our analysis, we found that the stiffer ships with large linear and nonlinear stiffness balance out large external wave forces.

Further, a comprehensive numerical analysis of the container ship reveals bifurcation structures that comprise multiple distinct regions with different behaviors. The governing parameters of the bifurcation structure are linear and nonlinear stiffness, damping, and excitation due to external wave force. For a certain set of parameters the system responses are periodic. This would be a well-behaved region which helps the designer to predict the trends accurately and without ambiguity. However, analyzing systematically for other parametric values, such as for lower values of linear stiffness, higher values of nonlinear stiffness, and higher values of external wave force corresponding to very rough, high, and very high sea states, the bifurcation structure reveals a mixed dynamic response in which periodic solutions evolve into period doubled, period tripled, and chaotic like solutions. This complex behavior persists for extremely high sea states (technically termed 'phenomenal') even when the damping is considerably higher.

Thus, in conclusion, the nonlinear single degree of freedom steering model derived in this paper is quite simple, robust, and efficient. This model can be

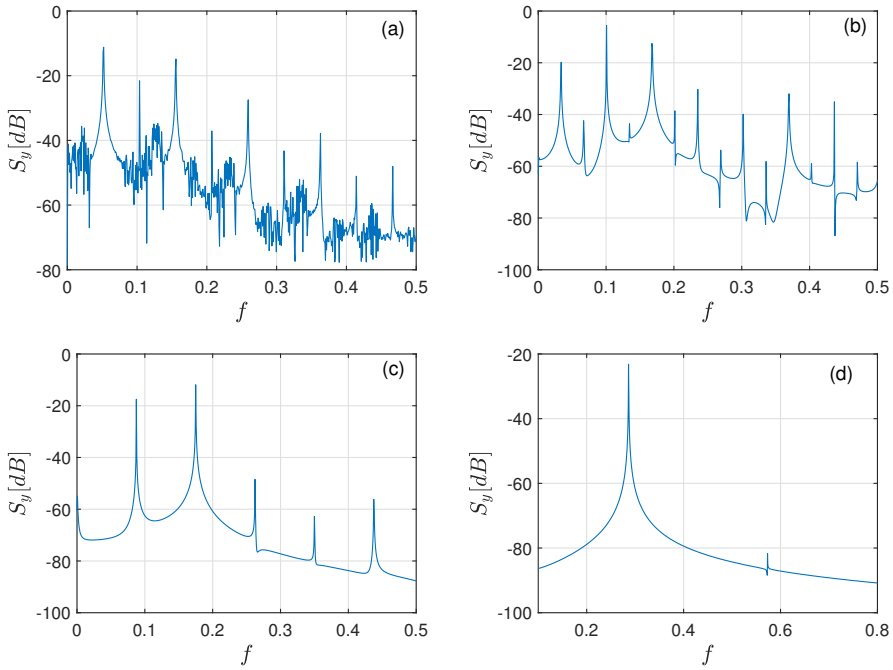

Fig. 10: Power spectra of a numerical simulation of Eq. (17) for a container ship for $\gamma = 0.05$, $\alpha_1 = 0.1$, $\alpha_2 = 0.5$, $\Delta = 0.01$, $F = 0.5$ corresponding to (a) $\Omega = 0.3255$ (b) $\Omega = 0.633$ (c) $\Omega = 1.1$ (d) $\Omega = 1.8$ in Fig. 6(b).

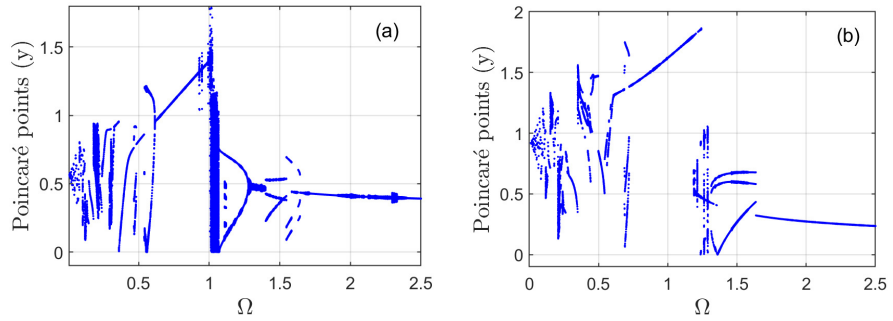

Fig. 11: Bifurcation diagram of a numerical simulation of Eq. (17) for a container ship for (a) $\gamma = 0.03$, $\alpha_1 = 0.05$, $\alpha_2 = 0.7$, $\Delta = 0.01$, $F = 0.3$. (b) $\gamma = 0.05$, $\alpha_1 = 0.05$, $\alpha_2 = 0.7$, $\Delta = 0.01$, $F = 0.6$.

further utilized to gain insights into the nonlinear dynamics of yaw motion of real ships and to design and implement smarter autopilots with much improved controllers for both non-autonomous and autonomous surface vehicles.

Statements and Declarations

Acknowledgements

CN and PK gratefully acknowledge the financial support from US Office of Naval Research (Grant: N00014-19-1-2070) for basic research on adaptive modeling of nonlinear dynamic systems. In particular, we appreciate the continuous encouragement from Capt. Lynn Petersen.

Conflict of Interest

The authors declare that they have no conflict of interest.

Data Availability

All data used in the study are openly available through Ref. [22, 34].

References

1. K. S. M. Davidson and L. I. Schiff, "Turning and course keeping qualities," *Transactions of SNAME*, vol. 54, 1946.
2. K. Nomoto, T. Taguchi, K. Honda, and S. Hirano, "On the steering qualities of ships," Tech. Rep., 1957.
3. M. A. Abkowitz, "Measurement of hydrodynamic characteristics from ship maneuvering trials by system identification," *Transactions-The Society of Naval Architects and Marine Engineers*, vol. 88, pp. 283–318, 1980.
4. T. I. Fossen and T. Lauvdal, "Nonlinear stability analysis of ship autopilots in sway, roll and yaw," in *Proceedings of the 3rd International Conference on Manoevring and Control of Marine Craft (MCMC,94)*, September 1994.
5. J. P. Strand and T. I. Fossen, "Nonlinear output feedback and locally optimal control of dynamically positioned ships: Experimental results."
6. O.-E. Fjellstad and T. I. Fossen, "Position and attitude tracking of AUVs. A quaternion feedback approach," *IEEE Journal of Oceanic Engineering*, vol. 19, no. 4, pp. 512–518, 1994.
7. R. Skjetne, O. N. Smogeli, and T. I. Fossen, "A nonlinear ship manoeuvering model: Identification and adaptive control with experiments for a model ship," *Modeling, Identification and Control*, vol. 25, no. 1, pp. 3–27, 2004.
8. R. Skjetne and T. I. Fossen, "Nonlinear maneuvering and control of ships," *IEEE*, pp. 1808–1815, 2001.
9. A. Loria, T. I. Fossen, and E. Panteley, "A separation principle for dynamic positioning of ships: Theoretical and experimental results," Tech. Rep. 2, March 2000.
10. K. Y. Pettersen and T. I. Fossen, "Underactauted dynamic positioning of a ship - experimental results," Tech. Rep. 5, September 2000.
11. T. I. Fossen and J. P. Strand, "Tutorial on nonlinear backstepping: Applications to ship control," Tech. Rep. 2, 1999.
12. T. I. Fossen and O.-E. Fjellstad, "Singularity-free tracking of unmanned underwater vehicles in 6 DOF," *Proceedings of the 33rd IEEE Conference on Decision and Control*, Dec 1999.
13. T. I. Fossen, "Recent development in ship control systems design," *World Superyacht Reveiw,Sterling Publications Limited, London*, 1999.
14. A. Loria, T. I. Fossen, and A. Teel, "UGAS and ULES of nonautonomous systems: Applications to integral control of ships and manipulators," Tech. Rep., December 1999.

15. T. I. Fossen, J.-M. Godhavn, S. P. Berge, and K. P. Lindegaard, "Nonlinear control of underactuated ships with forward speed compensation," Tech. Rep., 1998.
16. J. D. Hicks, A. W. Troesch, and C. Jiang, "Simulation and nonlinear dynamics analysis of planning hulls," *ASME Nonlinear Dynamics of Marine Vehicles*, vol. 1, pp. 41–55, November 1993.
17. S.-L. Chen, S. W. Shaw, and A. W. Troesch, "A systematic appraoch to modelling nonlinear multi-DOF ship motions in regular seas," *Journal of Ship Research*, vol. 43, no. 1, pp. 25–37, March 1999.
18. E. Lefeber, K. Y. Pettersen, and H. Nijmeijer, "Tracking control of an underactuated ship," *IEEE Transactions on Control Systems Technology*, vol. 11, no. 1, pp. 52–61, January 2003.
19. J. M. T. Thompson and S. R. Bishop, *Nonlinearity and Chaos in Engineering Dynamics.* Wiley, 1994.
20. F. C. Moon, *New Applications of Nonlinear and Chaotic Dynamics in Mechanics.* Dordrecht, Kluwer., 1999.
21. E. V. Lewis, "Principles of naval architecture, vol. III motion in waves and controllability," *Society of Naval Architects and Marine Engineers*, 1989.
22. K. H. Son and K. Nomoto, "On the coupled motion of steering and rolling of high speed container ship," *Journal of Society of Naval Architects, Japan*, vol. 150, pp. 232–244, 1981.
23. P. Oltmann, "Roll-an often neglected element of maneuvering." *International Conference on Marine Simulation and Maneuverability, New Foundland, Canada*, 1993.
24. C. Y. Tzeng, G. C. Goodwin, and S. Crisafulli, "Feedback linearisation design of a ship steering autopilot with saturating and slew rate limiting actuator," *International Journal of Adaptive Control and Signal Processing*, no. 13, pp. 23–30, 1999.
25. R. H. Akers, "Dynamic analysis of planing hulls in the vertical plane." *Proceedings of 1999 meeting of the New England Section of The Society of Naval Architects and Marine.*, pp. 1–19, 1999.
26. N. H. Norrbin, "Theory and observation on the use of a mathematical model for ship maneuvering in deep and conffined waters," *8^{th} Symposium on Naval Hydrodymanics, Pasadena, California*, 1970.
27. M. C. Fang and C. M. Liao, "Time simulation of nonlinear wave loads on a ship in oblique waves," *National Science Council*, vol. 21, pp. 454–465, 1997.
28. K. Spyrou, "Yaw stability of ships in steady wind," *Ship Technology Research*, vol. 42, 1995.
29. H. Yasukawa, T. Harino, Y. Nakayama, and K. K. Koh, "Course stability and yaw motion of a ship in steady wind," *Journal of Marine Science and Technology*, vol. 17, 2012.
30. C. Nataraj and R. Thimmaraya, "Tracking Control of Unmanned Surface Vehicles With Abkowitz Steering Model," vol. ASME 2010 Dynamic Systems and Control Conference, Volume 1, pp. 955–962, 09 2010. [Online]. Available: https://doi.org/10.1115/DSCC2010-4293
31. T. I. Fossen, *Guidance and Control of Ocean Vehicles.* New York, NY: John Wiley & Sons, 1994.
32. C. Kwuimy and C. Nataraj, "Nonlinear analysis of the yaw motion of a mariner vehicle under pd μ control," *Journal of Applied Nonlinear Dynamics*, vol. 6, pp. 531–545, 01 2017.
33. M. A. Abkowitz, "Lectures on ship hydrodynamics - steering and maneuverability," Hydro- and Aerodynamics Laboratory, Technical University of Denmark, Lyngby, Denmark, Tech. Rep. Hy-5, 1964.
34. S. Nomoto, "On the coupled motion of steering and rolling of a high speed container ship," *Naval Architect of Ocean Engineering, JSNA*, vol. 20, pp. 73–83, 1982.
35. MATLAB, "Matlab control toolbox release 2021a, the mathworks, inc., natick, massachusetts, united states," 2021. [Online]. Available: https://www.mathworks.com/help/control/ug/pid-controller-design-at-the-command-line.html
36. M. I. Bech and L. W. Smitt, "Analogue simulation of ship maneuvers based on full scale trials or free sailing model tests," Tech. Rep., 1969.
37. Wikipedia contributors, "Sea state — Wikipedia, the free encyclopedia," 2022, [Online; accessed 3-March-2022]. [Online]. Available: https://en.wikipedia.org/w/index.php?title=Sea_state&oldid=1070625922
38. J. J. Thompson, *Vibration and Stability.* Springer-Verlag Berlin Heidelberg, 2003.
39. W. Govaerts, Y. A. Kuznetsov, and B. Sautois, "MATCONT," *Scholarpedia*, vol. 1, no. 9, p. 1375, 2006, revision #123862.

Appendix

Notations and parameters:

m	mass
p	rolling rate
q	pitching rate
r	yawing rate
u	forward velocity (surge)
v	lateral velocity (sway)
w	vertical velocity (heave)
x	displacement along the x-axis in body-fixed coordinates
y	displacement along the y-axis in body-fixed coordinates
z	displacement along the z-axis in body-fixed coordinates
I	component of the moment of inertia tensor
K	moment component about the x-axis in body-fixed coordinates
M	moment component about the y-axis in body-fixed coordinates
N	moment component about the z-axis in body-fixed coordinates
X	force component along the x-axis in body-fixed coordinates
Y	force component along the y-axis in body-fixed coordinates
Z	force component along the z-axis in body-fixed coordinates
δ	rudder angle
ψ, θ, ϕ	Euler angles

Table 1: Data for a container ship. ℓ (Length of ship) = 175 m, U_0 (Initial surge) = 15 m/s [22, 34].

Parameter	Data	Parameter	Data	Parameter	Data	Parameter	Data	Parameter	Data
u_0	1	m	0.00792	x_G	0	I_{yz}	0	$N_{rr\delta}$	0
I_{xx}	0.0000176	I_{yy}	0	I_{zz}	+45.6e-5	I_{xy}	0	$N_{\delta\delta v}$	0
I_{zx}	0	I_{zy}	0	X_0	0	$X_{\dot{u}}$	0	N_{vuu}	0
X_u	0	X_{uu}	-0.0004226	X_{uuu}	0	X_{vv}	-0.00386	$N_{\delta uu}$	0
X_{rr}	+0.00020	$X_{\delta\delta}$	0	X_{rv}	-0.00311	$X_{r\delta}$	0	$N_{\delta\delta r}$	0
$X_{v\delta}$	0	X_{vvu}	0	X_{rru}	0	$X_{\delta\delta u}$	0	$N_{vv\delta}$	0
X_{rvu}	0	$X_{r\delta u}$	0	$X_{v\delta u}$	0	$X_{\dot{v}}$	0	N_{ru}	0
$X_{\dot{w}}$	0	$X_{\dot{p}}$	0	$X_{\dot{q}}$	0	$X_{\dot{r}}$	0	$N_{\dot{p}}$	0
Y_0	0	Y_u	0	Y_{uu}	0	Y_r	0.00242	N_{rrv}	0
Y_v	-1160e – 5	$Y_{\dot{r}}$	0	$Y_{\dot{v}}$	0	Y_δ	-.002578	$N_{\delta vr}$	0
Y_{rrr}	0.00177	Y_{vvv}	-0.109	$Y_{\delta\delta\delta}$	0	$Y_{rr\delta}$	0	N_{ruu}	0
$Y_{\delta\delta r}$	0	Y_{rrv}	-0.0405	Y_{vvr}	0.0214	$Y_{\delta\delta v}$	0	$N_{\dot{q}}$	0
$Y_{vv\delta}$	0	$Y_{\delta vr}$	0	Y_{vu}	0	Y_{vuu}	0	N_{vvr}	0
Y_{ru}	0	Y_{ruu}	0	$Y_{\delta u}$	0	$Y_{\delta uu}$	0	N_{vu}	0
$Y_{\dot{p}}$	0	$Y_{\dot{q}}$	0	$Y_{\dot{w}}$	0	$Z_{\dot{w}}$	0	$N_{\delta u}$	0
$K_{\dot{p}}$	0	$M_{\dot{p}}$	0	$Z_{\dot{p}}$	0	$K_{\dot{q}}$	0	-	-
$M_{\dot{q}}$	0	$Z_{\dot{q}}$	0	$K_{\dot{r}}$	0	$M_{\dot{r}}$	0	-	-
$Z_{\dot{r}}$	0	N_0	0	N_u	0	N_{uu}	0	-	-
N_r	-0.00242	N_v	-0.0038545	$N_{\dot{r}}$	0	$N_{\dot{v}}$	0	-	-
N_δ	0.00126	N_{rrr}	-0.00229	N_{vvv}	0.001492	$N_{\delta\delta\delta}$	0	-	-

Coefficients of Nomoto's 2^{nd} order model (Eq. (9)):

$$K = \frac{-\Big(N(2,1)b(1,1) - N(1,1)b(2,1)\Big)}{\det(N)}, \tag{27}$$

$$T_3 = \frac{(M(2,1)b(1,1) - M(1,1)b(2,1))}{(K\det(N))}, \tag{28}$$

$$A = \frac{\det(M)}{\det(N)}, \tag{29}$$

$$B = \frac{\Big(N(1,1)M(2,2) + N(2,2)M(1,1) - N(1,2)M(2,1) - N(2,1)M(1,2)\Big)}{\det(N)}, \tag{30}$$

$$C = \sqrt{(B^2 - 4A)}, \tag{31}$$

$$T_1 = \frac{(B+C)}{2}, \tag{32}$$

$$T_2 = B - T_1, \tag{33}$$

where,

$$M = \begin{bmatrix} m - Y_{\dot{v}} & mx_G - Y_{\dot{r}} \\ mx_G - N_{\dot{v}} & I_z - N_{\dot{r}} \end{bmatrix} \qquad N_{u_0} = \begin{bmatrix} -Y_v & mu_0 - Y_r \\ -N_v & mx_G u_0 - N_r \end{bmatrix} \qquad b = \begin{bmatrix} Y_\delta \\ N_\delta \end{bmatrix}$$

Table 2: Constants of 2^{nd} order Nomoto's model using parameters in Tab. 1 and Eqs. (27)-(33).

T_1	T_2	T_3	K
3.4043	0.1544	-0.4064	3.5728

Coefficients of Eq. (15):

$$\begin{aligned} a_{11} &= \Big(1 - \frac{K}{T_1 T_2} k_d T_3\Big) \\ a_{12} &= \left[\Big(\frac{1}{T_1} + \frac{1}{T_2}\Big) + \frac{K}{T_1 T_2}\left(k_p T_3 - k_d\right)\right] \\ a_{13} &= \frac{K}{T_1 T_2}\left(a + k_p\right),\ a_{14} = b\frac{K}{T_1 T_2},\ a_{15} = c\frac{K}{T_1 T_2},\ a_{16} = d\frac{K}{T_1 T_2} \end{aligned} \tag{34}$$

Table 3: Sea states [37], and nondimensional wave amplitude.

Sea states	Wave height (meters)	$F = \frac{f a_{15}^{\frac{1}{4}}}{a_{11} b_{11}}$
Calm	0 to 0.1	0 to 0.0036
Smooth	0.1 to 0.5	0.0036 to 0.018
Slight	0.5 to 1.25	0.018 to 0.045
Moderate	1.25 to 2.5	0.045 to 0.09
Rough	2.5 to 4	0.09 to 0.14
Very rough	4 to 6	0.14 to 0.21
High	6 to 9	0.21 to 0.32
Very high	9 to 14	0.32 to 0.5
Phenomenal	above 14	above 0.5